Journal of Organometallic Chemistry 696 (2011) 4112–4120

Contents lists available at ScienceDirect

Journal of Organometallic Chemistry

journal homepage: www.elsevier.com/locate/jorganchem

Synthesis, characterization and photovoltaic properties of platinum-containing poly(aryleneethynylene) polymers with phenanthrenyl-imidazole moiety

Hongmei Zhan [a], Wai-Yeung Wong [a,*,1], Annie Ng [b], Aleksandra B. Djurišić [b,**], Wai-Kin Chan [c]

[a] Institute of Molecular Functional Materials,[1] Department of Chemistry and Centre for Advanced Luminescence Materials, Hong Kong Baptist University, Waterloo Road, Kowloon Tong, Hong Kong, PR China
[b] Department of Physics, The University of Hong Kong, Pokfulam Road, Hong Kong, PR China
[c] Department of Chemistry, The University of Hong Kong, Pokfulam Road, Hong Kong, PR China

ARTICLE INFO

Article history:
Received 21 May 2011
Received in revised form
4 July 2011
Accepted 4 July 2011

Keywords:
Phenanthrenyl-imidazole
Solar cell
Platinum
Thiophene
Metallopolymer

ABSTRACT

A new type of soluble, solution-processable platinum(II) polyyne polymers based on phenanthrenyl-imidazole chromophore and their corresponding diplatinum model complexes were synthesized via the CuI-catalyzed dehydrohalogenation reaction of the platinum(II) chloride precursor and each of the diethynyl ligands. The photophysical (absorption and emission spectra), thermal, electrochemical and photovoltaic properties of the polymers were investigated. Both polymers exhibit strong absorption bands centered at 459–466 nm. The effect of adding thiophene ring along the polymer backbone was evaluated. Bulk heterojunction solar cells fabricated by blending these metallopolymers with methanofullerene were studied, with the power conversion efficiency reaching 0.39%, although the band gap energies of the polymers are not low.

© 2011 Elsevier B.V. All rights reserved.

1. Introduction

In recent years, organic solar cells (OSCs) have received a great deal of attention in academic and industrial laboratories due to their advantages such as low cost, light weight, solution-based processing and flexible devices [1–4]. Conjugated polymers possessing delocalized π-electron systems have been studied extensively for their application in bulk heterojunction (BHJ) solar cells, in which the photoactive thin film consists of a bicontinuous and interpenetrating blend of polymeric donors and fullerene acceptors [5]. The power conversion efficiency (PCE) of OSCs has reached up to ~7–8% [6,7]. For fulfilling the goal of large scale commercialization as a renewable energy source, the photovoltaic efficiencies of OSCs must be further enhanced. So, it is necessary to design and develop new donor materials possessing better absorption properties in the visible spectrum and high charge carrier mobilities.

In order to harvest more photons and further improve the photovoltaic efficiencies of OSCs, key developments have focused on narrowing the polymer band gap. One of the most effective approaches is designing the conjugated polymers containing electron donor–acceptor (D–A) pairs. Intramolecular D–A systems can enhance the rate of charge transfer within molecules or polymers [8–13]. There are two kinds of D–A systems: one possesses alternating electron-rich donor and electron-deficient acceptor units along the polymer main chains, which are usually encountered in BHJ solar cells and have shown promising performance with the PCE as high as ~3–7% [6,7,14–21]; the other typical architecture is the electron-deficient acceptor unit as the side chain attached to the conjugated polymer backbone in a coplanar manner [22–26]. The introduction of an electron acceptor unit as side chain to the polymeric main chain can also effectively widen the absorption band and enhance charge transfer ability. This molecular architecture used in BHJ device has the advantage that it allows charge separation through sequential transfer of electrons from the main chains to the side chains and then to methanofullerene such as [6,6]-phenyl C_{61}-butyric acid methyl ester (PCBM) [22,23,27]. Phenanthrenyl-imidazole is a π-conjugated and planar structure, and the imidazole is an electron-deficient ring used as an acceptor unit.. Recently, Wei and co-workers reported a series of phenanthrenyl-imidazole-containing regioregular polythiophene copolymers, which showed relatively better performance with PCE of ~2.8–4.1% [22–24]. In addition, metal-containing conjugated organic polymers represent an intriguing and promising class of

* Corresponding author. Tel.: +852 34117074; fax: +852 34117348.
** Corresponding author. Tel.: +852 28597946; fax: +852 25599152.
E-mail addresses: rwywong@hkbu.edu.hk (W.-Y. Wong), dalek@hku.hk (A.B. Djurišić).
[1] Areas of Excellence Scheme, University Grants Committee (Hong Kong).

0022-328X/$ – see front matter © 2011 Elsevier B.V. All rights reserved.
doi:10.1016/j.jorganchem.2011.07.005

materials, and platinum alkynyls have been a popular candidate for inclusion into such a polymeric backbone owing to their potential applications in molecular electronics and materials science, especially the platinum metallopolyyne polymers of the general form *trans*-[-Pt(L)$_2$C≡CRC≡C-]$_n$ (L is an auxiliary phosphine ligand, and R is an aromatic spacer unit). The d-orbital of the platinum can overlap with the p-orbital of the alkyne unit, and hence enhance the π-conjugation and π-electron delocalization along the polymer backbone [28]. Furthermore, efficient intersystem crossing in such organometallic species facilitates the formation of triplet excited states and thus allows extended exciton diffusion lengths [29–35]. These features enable these metallopolymers to be used as the donor materials in photovoltaic cells, and the mean PCE of 4.1% has been achieved by the platinum metallopolyyne polymers based on the benzothiadiazole chromophore [36–38]. The work was also extended to other heterocyclic spacers [39–43].

In view of the considerations above, we report here the synthesis, characterization and photovoltaic properties of two platinum metallopolyyne polymers based on thiophene chromophore and the electron-deficient phenanthrenyl-imidazole attached to the thiophene unit as a side chain. The hexyl groups would improve the solubilities of the polymers. Compared with **P1**, polymer **P2** possesses two additional thiophene rings in one building block unit, which is expected to further improve the absorption properties of polymers and thus enhance the performance of polymer solar cells.

2. Experimental

2.1. General information

All reactions were carried out under a nitrogen atmosphere by using standard Schlenk techniques. Solvents were dried and distilled from appropriate drying agents under an inert atmosphere prior to use. Glassware was oven-dried at about 120 °C. All reagents and chemicals, unless otherwise stated, were purchased from commercial sources and used without further purification. *trans*-Pt(PEt$_3$)$_2$(Ph)Cl [44] and *trans*-Pt(PBu$_3$)$_2$Cl$_2$ [45] were prepared according to the literature methods. All reactions were monitored by thin-layer chromatography (TLC) with Merck pre-coated glass plates. Flash column chromatography and preparative TLC were carried out using silica gel from Merck (230–400 mesh). Infrared spectra were recorded as CH_2Cl_2 solutions using a Perkin–Elmer Paragon 1000 PC or Nicolet Magna 550 Series II FTIR spectrometer, using CaF_2 cells with a 0.5 mm path length. Fast atom bombardment (FAB) mass spectra were recorded on a Finnigan MAT SSQ710 system and MALDI-TOF (matrix-assisted laser desorption/ionization time-of-flight) spectra were obtained by an Autoflex Bruker MALDI-TOF mass spectrometer. NMR spectra were measured in $CDCl_3$ on a Varian Inova 400 MHz FT-NMR spectrometer and chemical shifts are quoted relative to tetramethylsilane for ^{1}H and ^{13}C nuclei and H_3PO_4 for ^{31}P nucleus.

2.2. Physical measurements

UV/vis spectra were obtained on an HP-8453 diode array spectrophotometer. The solution emission spectra and lifetimes of the compounds were measured on a Photon Technology International (PTI) Fluorescence QuantaMaster Series QM1 spectrophotometer. The quantum yields were determined in degassed CH_2Cl_2 solutions at 293 K against coumarin 6 in ethanol ($\Phi_F = 0.78$) [46]. The cyclic voltammetry measurements were carried out at a scan rate of 100 mV s^{-1} using a eDAQ EA161 potentiostat electrochemical interface equipped with a thin film coated ITO covered glass working electrode, a platinum counter electrode and a Ag/AgCl (in 3 M KCl) reference electrode. The solvent in all measurements was deoxygenated acetonitrile, and the supporting electrolyte was 0.1 M [^{n}Bu$_4$N]BF$_4$. Thin polymer films were deposited on the working electrode by dip-coating in chlorobenzene solution (6 mg mL^{-1}). Where appropriate, the oxidation and reduction potentials were used to determine the HOMO and LUMO energy levels using the equations $E_{HOMO} = [-(E_{ox\ (vs.\ Ag/AgCl)} - E_{(N.H.E.\ vs.\ Ag/AgCl)})] - 4.50$ eV and $E_{LUMO} = [-(E_{red\ (vs.\ Ag/AgCl)} - E_{(N.H.E.\ vs.\ Ag/AgCl)})] - 4.50$ eV, where the potentials for N.H.E. vs. vacuum and N.H.E. vs. Ag/AgCl are 4.50 and −0.22 V, respectively [47,48]. The molecular weights of the polymers were determined by GPC (HP 1050 series HPLC with visible wavelength and fluorescent detectors) using polystyrene standards. Thermal analyses were performed with a Perkin–Elmer TGA6 thermal analyzer.

2.3. Preparation of compounds

2.3.1. Synthesis of ***PITBr***

A mixture of phenanthrenequinone (0.83 g, 4 mmol), 2,5-dibromo-3-thiophene-carboxaldehyde (1.07 g, 4 mmol), aniline (1.86 g, 20 mmol), ammonium acetate (1.23 g, 16 mmol), and glacial acetic acid (25 mL) was charged sequentially in a single-necked flask and heated in an oil bath to a bath temperature of 123 °C under nitrogen, maintained at this temperature for 3–5 h. After cooling, the solvent was removed under reduced pressure. The residue was dissolved in CH_2Cl_2 (75 mL) and then the solution was washed with water and brine. Organic layer was dried by Na_2SO_4, filtered and concentrated under reduced pressure. The residue was purified by silica gel column chromatography to give the crude product, which was then recrystallized from the mixture solution of CH_2Cl_2 and hexane to obtain the pure product **PITBr** (1.21 g, 57%) as a wheat-yellow powder.

Spectral data: ^{1}H NMR (400 MHz, $CDCl_3$, δ/ppm): 8.82 (dd, $J_1 = 8.0$ Hz, $J_2 = 1.0$ Hz, 1H, Ar), 8.77 (d, $J = 8.4$ Hz, 1H, Ar), 8.70 (d, $J = 8.2$ Hz, 1H, Ar), 7.74 (t, $J = 7.0$ Hz, 1H, Ar), 7.68–7.64 (m, 1H, Ar), 7.60–7.57 (m, 4H, Ar), 7.48–7.46 (m, 2H, Ar), 7.30–7.27 (m, 1H, Ar), 7.25–7.22 (m, 1H, Ar), 6.76 (s, 1H, Ar); ^{13}C NMR (100 MHz, $CDCl_3$, δ/ppm): 144.27, 137.36, 137.23, 132.27, 131.49, 129.91, 129.89, 129.37, 128.34, 128.28, 127.48, 127.42, 127.04, 126.36, 125.79, 125.28, 124.10, 123.11, 122.71, 122.66, 120.96, 114.82, 111.33 (Ar); FAB-MS: m/z 535.0 [M]$^+$.

2.3.2. Synthesis of ***L1-HT***

To a solution of 2-(2,5-dibromothiophen-3-yl)-1-phenyl-1*H*-phenanthro[9,10-*d*]imidazole (**PITBr**, 0.27 g, 0.5 mmol) and tributyl(4-hexyl-thiophen-2-yl)stannane (0.73 g, 1.6 mmol) in dry toluene (10 mL) under nitrogen was added the catalyst Pd(PPh$_3$)$_4$ (29 mg, 0.025 mmol). The reaction mixture was heated to reflux for 1 day until reaction completion as shown by TLC analysis. The reaction mixture was cooled to room temperature and the solvent was removed. The residue was purified by column chromatography on silica gel eluting with CH_2Cl_2/hexane (1.5:1, v/v) to give the compound **L1-HT** (0.32 g, 84%) as an orange solid.

Spectral data: ^{1}H NMR (400 MHz, $CDCl_3$, δ/ppm): 8.87 (dd, $J_1 = 8.0$ Hz, $J_2 = 1.2$ Hz, 1H, Ar), 8.77 (d, $J = 8.4$ Hz, 1H, Ar), 8.72 (d, $J = 8.3$ Hz, 1H, Ar), 7.77–7.73 (m, 1H, Ar), 7.68–7.64 (m, 1H, Ar), 7.53–7.49 (m, 1H, Ar), 7.44–7.40 (m, 1H, Ar), 7.36–7.32 (m, 2H, Ar), 7.26–7.24 (m, 1H, Ar), 7.22–7.19 (m, 2H, Ar), 7.09–7.07 (m, 2H, Ar), 6.97 (d, $J = 1.3$ Hz, 1H, Ar), 6.80 (d, $J = 1.0$ Hz, 1H, Ar), 6.72 (d, $J = 1.3$ Hz, 1H, Ar), 6.69 (s, 1H, Ar), 2.56 (t, $J = 7.5$ Hz, 2H, C$_6$H$_{13}$), 2.41 (t, $J = 7.5$ Hz, 2H, C$_6$H$_{13}$), 1.64–1.57 (m, 2H, C$_6$H$_{13}$), 1.46–1.38 (m, 2H, C$_6$H$_{13}$), 1.37–1.28 (m, 6H, C$_6$H$_{13}$), 1.23–1.09 (m, 6H, C$_6$H$_{13}$), 0.89 (t, $J = 6.6$ Hz, 3H, C$_6$H$_{13}$), 0.82 (t, $J = 6.8$ Hz, 3H, C$_6$H$_{13}$); ^{13}C NMR (100 MHz, $CDCl_3$, δ/ppm): 146.86, 144.18, 143.66, 137.42, 137.38, 136.74, 136.05, 135.62, 134.67, 129.28, 129.08, 128.27, 127.93, 127.61,

127.49, 127.34, 127.30, 126.94, 126.46, 126.23, 125.63, 125.31, 125.06, 124.05, 123.13, 122.86, 122.83, 121.11, 121.04, 119.55 (Ar), 31.54, 30.45, 30.35, 30.26, 29.00, 28.83, 28.28, 26.79, 22.53, 17.31, 14.12, 13.66 (C_6H_{13}); FAB-MS: *m*/*z* 709.4 $[M]^+$.

2.3.3. Synthesis of ***L1-Br***

Compound **L1-HT** (0.11 g, 0.15 mmol) was dissolved in THF (10 mL). NBS (55 mg, 0.31 mmol) was then added to the solution and the mixture was stirred overnight at room temperature in the dark. Until the reaction completion as shown by TLC analysis, the solvent was removed. The residue was purified by column chromatography on silica gel eluting with CH_2Cl_2/hexane (1:1, v/v) to give the pure compound **L1-Br** (0.10 g, 75%) as an orange solid.

Spectral data: ^{1}H NMR (400 MHz, $CDCl_3$, δ/ppm): 8.86 (d, $J = 7.9$ Hz, 1H, Ar), 8.74 (d, $J = 8.4$ Hz, 1H, Ar), 8.69 (d, $J = 8.4$ Hz, 1H, Ar), 7.74 (t, $J = 7.8$ Hz, 1H, Ar), 7.64 (t, $J = 7.7$ Hz, 1H, Ar), 7.51–7.42 (m, 2H, Ar), 7.37 (t, $J = 7.8$ Hz, 2H, Ar), 7.23–7.20 (m, 2H, Ar), 7.14 (d, $J = 7.3$ Hz, 2H, Ar), 7.05 (s, 1H, Ar), 6.80 (s, 1H, Ar), 6.67 (s, 1H, Ar), 2.49 (t, $J = 7.5$ Hz, 2H, C_6H_{13}), 2.37 (t, $J = 7.5$ Hz, 2H, C_6H_{13}), 1.57–1.52 (m, 2H, C_6H_{13}), 1.41–1.30 (m, 8H, C_6H_{13}), 1.19–1.07 (m, 6H, C_6H_{13}), 0.89 (t, $J = 6.9$ Hz, 3H, C_6H_{13}), 0.79 (t, $J = 6.8$ Hz, 3H, C_6H_{13}); ^{13}C NMR (100 MHz, $CDCl_3$, δ/ppm): 145.70, 143.16, 142.63, 137.47, 137.39, 136.06, 135.62, 134.89, 134.24, 129.54, 129.44, 129.32, 128.38, 127.99, 127.57, 127.43, 127.42, 127.40, 127.24, 126.75, 126.31, 125.77, 125.23, 124.94, 124.14, 123.18, 122.84, 122.80, 121.10, 110.40, 108.27 (Ar), 31.64, 31.48, 29.63, 29.37, 28.94, 28.78, 22.63, 22.51, 21.09, 14.52, 14.16, 14.11 (C_6H_{13}); FAB-MS: *m*/*z* 867.0 $[M]^+$.

2.3.4. Synthesis of ***L2-T***

The procedure was similar to that of **L1-HT**.

Orange solid (77%). *Spectral data*: ^{1}H NMR (400 MHz, $CDCl_3$, δ/ppm): 8.89 (dd, $J_1 = 8.0$ Hz, $J_2 = 1.1$ Hz, 1H, Ar), 8.76 (d, $J = 8.6$ Hz, 1H, Ar), 8.71 (d, $J = 8.3$ Hz, 1H, Ar), 7.77–7.73 (m, 1H, Ar), 7.68–7.64 (m, 1H, Ar), 7.52–7.35 (m, 4H, Ar), 7.30–7.28 (m, 1H, Ar), 7.24–7.10 (m, 7H, Ar), 7.06–7.04 (m, 1H, Ar), 6.98 (s, 1H, Ar), 6.95–6.92 (m, 2H, Ar), 6.74 (s, 1H, Ar), 2.70 (t, $J = 7.8$ Hz, 2H, C_6H_{13}), 2.55 (t, $J = 7.7$ Hz, 2H, C_6H_{13}), 1.65–1.61 (m, 2H, C_6H_{13}), 1.42–1.30 (m, 8H, C_6H_{13}), 1.10–1.00 (m, 6H, C_6H_{13}), 0.89–0.86 (m, 3H, C_6H_{13}), 0.75 (t, $J = 7.2$ Hz, 3H, C_6H_{13}); ^{13}C NMR (100 MHz, $CDCl_3$, δ/ppm): 146.26, 140.47, 140.08, 137.51, 137.41, 136.16, 135.65, 135.46, 135.25, 134.09, 132.62, 131.58, 130.27, 129.45, 129.38, 129.34, 129.18, 128.34, 128.01, 127.52, 127.49, 127.42, 127.39, 127.28, 126.84, 126.81, 126.26, 126.08, 125.67, 125.61, 125.55, 125.12, 124.11, 123.15, 122.86, 121.12 (Ar), 31.68, 31.46, 30.57, 30.49, 29.34, 29.27, 29.11, 29.07, 22.65, 22.48, 14.19, 14.09 (C_6H_{13}); FAB-MS: *m*/*z* 873.2 $[M]^+$.

2.3.5. Synthesis of ***L2-Br***

The procedure was similar to that of **L1-Br**.

L2-Br: Orange solid (88%). *Spectral data*: ^{1}H NMR (400 MHz, $CDCl_3$, δ/ppm): 8.89 (dd, $J_1 = 8.0$ Hz, $J_2 = 1.2$ Hz, 1H, Ar), 8.75 (d, $J = 8.6$ Hz, 1H, Ar), 8.70 (d, $J = 8.4$ Hz, 1H, Ar), 7.76–7.72 (m, 1H, Ar), 7.67–7.63 (m, 1H, Ar), 7.51–7.42 (m, 2H, Ar), 7.38–7.35 (m, 2H, Ar), 7.24–7.21 (m, 2H, Ar), 7.17–7.13 (m, 3H, Ar), 6.98 (d, $J = 3.9$ Hz, 1H, Ar), 6.95 (s, 1H, Ar), 6.87 (d, $J = 3.8$ Hz, 1H, Ar), 6.83 (d, $J = 3.9$ Hz, 1H, Ar), 6.75 (s, 1H, Ar), 6.66 (d, $J = 3.9$ Hz, 1H, Ar), 2.64 (t, $J = 7.8$ Hz, 2H, C_6H_{13}), 2.50 (t, $J = 7.6$ Hz, 2H, C_6H_{13}), 1.62–1.58 (m, 2H, C_6H_{13}), 1.39–1.29 (m, 8H, C_6H_{13}), 1.12–1.01 (m, 6H, C_6H_{13}), 0.88–0.85 (m, 3H, C_6H_{13}), 0.76 (t, $J = 7.3$ Hz, 3H, C_6H_{13}); ^{13}C NMR (100 MHz, $CDCl_3$, δ/ppm): 145.94, 140.93, 140.49, 137.44, 137.31, 137.03, 136.81, 136.02, 135.06, 134.43, 132.99, 130.69, 130.25, 130.16, 129.41, 129.33, 129.26, 129.19, 129.16, 128.28, 127.91, 127.45, 127.43, 127.33, 127.17, 126.94, 126.74, 126.21, 125.66, 125.11, 124.05, 123.10, 122.74, 121.03, 112.10, 112.05 (Ar), 31.57, 31.38, 30.48, 30.41, 29.24, 29.17, 29.02, 28.98, 22.58, 22.41, 14.10, 14.03 (C_6H_{13}); FAB-MS: *m*/*z* 1031.2 $[M]^+$.

2.3.6. Synthesis of ***L1-TMS*** and ***L2-TMS***

To an ice-cooled mixture of **L1-Br** (99 mg, 0.11 mmol) in dry triethylamine (6 mL) and CH_2Cl_2 (6 mL) solution mixture were added CuI (3.8 mg, 0.02 mmol), $Pd(OAc)_2$ (4.5 mg, 0.02 mmol) and PPh_3 (16 mg, 0.06 mmol). After the solution was stirred for 30 min at 0 °C, trimethylsilylacetylene (54 mg, 0.55 mmol) was then added and the suspension was stirred for 30 min in an ice-bath before being warmed to room temperature. After reacting for 30 min at room temperature, the mixture was refluxed for 20 h. The solution was then allowed to cool to room temperature and the solvent mixture was evaporated *in vacuo*. The residue was purified by column chromatography on silica gel eluting with a solvent combination of CH_2Cl_2/hexane (1:2, v/v) to provide **L1-TMS** (72 mg, 70%) as an orange solid.

Spectral data: ^{1}H NMR (400 MHz, $CDCl_3$, δ/ppm): 8.86 (dd, $J_1 = 8.0$ Hz, $J_2 = 1.1$ Hz, 1H, Ar), 8.76 (d, $J = 8.4$ Hz, 1H, Ar), 8.71 (d, $J = 8.3$ Hz, 1H, Ar), 7.74 (t, $J = 7.1$ Hz, 1H, Ar), 7.65 (t, $J = 7.7$ Hz, 1H, Ar), 7.52–7.48 (m, 1H, Ar), 7.46–7.42 (m, 1H, Ar), 7.38–7.35 (m, 2H, Ar), 7.26–7.19 (m, 2H, Ar), 7.16–7.13 (m, 3H, Ar), 6.86 (s, 1H, Ar), 6.68 (s, 1H, Ar), 2.63 (t, $J = 7.5$ Hz, 2H, C_6H_{13}), 2.51 (t, $J = 7.4$ Hz, 2H, C_6H_{13}), 1.62–1.59 (m, 2H, C_6H_{13}), 1.45–1.41 (m, 2H, C_6H_{13}), 1.36–1.31 (m, 6H, C_6H_{13}), 1.23–1.11 (m, 6H, C_6H_{13}), 0.89 (t, $J = 6.9$ Hz, 3H, C_6H_{13}), 0.81 (t, $J = 6.8$ Hz, 3H, C_6H_{13}), 0.25 (s, 9H, TMS), 0.16 (s, 9H, TMS); ^{13}C NMR (100 MHz, $CDCl_3$, δ/ppm): 149.90, 149.44, 145.88, 137.60, 137.44, 136.62, 135.96, 135.33, 134.59, 129.63, 129.49, 129.43, 128.43, 128.08, 127.76, 127.75, 127.53, 127.38, 127.35, 127.30, 126.42, 125.85, 125.31, 125.08, 124.23, 123.27, 122.97, 122.93, 121.18, 119.45, 117.92 (Ar), 103.05, 102.82, 97.22, 97.11 (C≡C), 31.68, 31.55, 30.08, 30.01, 29.68, 29.45, 29.02, 28.88, 22.72, 22.62, 14.26, 14.22 (C_6H_{13}), 0.07, −0.00 (TMS); FAB-MS: *m*/*z* 901.5 $[M]^+$. Anal. Calc. for $C_{55}H_{60}N_2S_3Si_2$: C, 73.28; H, 6.71; N, 3.11. Found: C, 73.55; H, 6.82; N, 3.32%.

The same procedure was used to prepare **L2-TMS**.

L2-TMS: Orange solid (91%). ^{1}H NMR (400 MHz, $CDCl_3$, δ/ppm): 8.86 (d, $J = 7.9$ Hz, 1H, Ar), 8.78 (d, $J = 8.4$ Hz, 1H, Ar), 8.73 (d, $J = 8.4$ Hz, 1H, Ar), 7.76 (t, $J = 7.1$ Hz, 1H, Ar), 7.70 (t, $J = 7.0$ Hz, 1H, Ar), 7.54–7.50 (m, 1H, Ar), 7.46 (t, $J = 7.5$ Hz, 1H, Ar), 7.38 (t, $J = 7.8$ Hz, 2H, Ar), 7.26–7.22 (m, 2H, Ar), 7.17–7.15 (m, 4H, Ar), 7.05 (d, $J = 3.8$ Hz, 1H, Ar), 6.97 (s, 1H, Ar), 6.95 (d, $J = 3.8$ Hz, 1H, Ar), 6.78 (d, $J = 3.8$ Hz, 1H, Ar), 6.75 (s, 1H, Ar), 2.71 (t, $J = 7.8$ Hz, 2H, C_6H_{13}), 2.55 (t, $J = 7.7$ Hz, 2H, C_6H_{13}), 1.65–1.61 (m, 2H, C_6H_{13}), 1.42–1.31 (m, 8H, C_6H_{13}), 1.19–1.01 (m, 6H, C_6H_{13}), 0.90 (t, $J = 6.5$ Hz, 3H, C_6H_{13}), 0.76 (t, $J = 7.0$ Hz, 3H, C_6H_{13}), 0.26 (s, 9H, TMS), 0.22 (s, 9H, TMS); ^{13}C NMR (100 MHz, $CDCl_3$, δ/ppm): 146.11, 141.22, 140.81, 137.58, 137.46, 137.36, 137.15, 136.18, 135.23, 134.54, 133.19, 133.10, 131.27, 129.81, 129.65, 129.58, 129.49, 129.33, 128.45, 128.07, 127.63, 127.59, 127.50, 127.32, 127.14, 126.39, 125.81, 125.81, 125.54, 125.27, 124.21, 123.26, 123.01, 122.98, 122.91, 121.21 (Ar), 100.45, 100.37, 97.41, 97.36 (C≡C), 31.76, 31.54, 30.52, 30.43, 29.61, 29.35, 29.15, 22.73, 22.55, 14.24, 14.17 (C_6H_{13}), −0.01, −0.05 (TMS); FAB-MS: *m*/*z* 1065.5 $[M]^+$. Anal. Calc. for $C_{63}H_{64}N_2S_5Si_2$: C, 71.01; H, 6.05; N, 2.63. Found: C, 71.32; H, 5.97; N, 2.78%.

2.3.7. Synthesis of ***L1*** and ***L2***

To a solution of **L1-TMS** (68 mg, 0.075 mmol) in CH_2Cl_2 (5 mL) and MeOH (5 mL) was added K_2CO_3 (22 mg, 0.158 mmol), and the solution was stirred at room temperature for 6 h under nitrogen. After the reaction was complete as shown by TLC analysis, the solvent was removed under reduced pressure. The residue was purified by column chromatography on silica gel using CH_2Cl_2/hexane (1.5:1, v/v) as eluent to afford compound **L1** (40 mg, 71%) as an orange solid.

Spectral data: IR (KBr): ν(C≡C) 2094 cm^{-1}; ^{1}H NMR (400 MHz, $CDCl_3$, δ/ppm): 8.85 (dd, $J_1 = 7.9$ Hz, $J_2 = 1.2$ Hz, 1H, Ar), 8.77 (d, $J = 8.4$ Hz, 1H, Ar), 8.73 (d, $J = 8.2$ Hz, 1H, Ar), 7.77–7.73 (m, 1H, Ar),

7.69–7.65 (m, 1H, Ar), 7.54–7.50 (m, 1H, Ar), 7.47–7.43 (m, 1H, Ar), 7.40–7.36 (m, 2H, Ar), 7.27–7.20 (m, 2H, Ar), 7.16–7.14 (m, 3H, Ar), 6.89 (s, 1H, Ar), 6.70 (s, 1H, Ar), 3.51 (s, 1H, C≡CH), 3.39 (s, 1H, C≡CH), 2.65 (t, $J = 7.5$ Hz, 2H, C_6H_{13}), 2.52 (t, $J = 7.5$ Hz, 2H, C_6H_{13}), 1.64–1.57 (m, 2H, C_6H_{13}), 1.45–1.38 (m, 2H, C_6H_{13}), 1.34–1.30 (m, 6H, C_6H_{13}), 1.22–1.09 (m, 6H, C_6H_{13}), 0.89 (t, $J = 6.5$ Hz, 3H, C_6H_{13}), 0.79 (t, $J = 6.8$ Hz, 3H, C_6H_{13}); ^{13}C NMR (100 MHz, $CDCl_3$, δ/ppm): 150.10, 149.51, 145.63, 137.47, 137.31, 136.38, 136.20, 135.16, 134.86, 129.52, 129.42, 129.33, 128.35, 127.93, 127.87, 127.62, 127.42, 127.30, 127.24, 127.21, 126.30, 125.74, 125.22, 124.92, 124.11, 123.16, 122.82, 122.78, 121.08, 118.01, 116.55 (Ar), 84.93, 84.75, 76.32, 72.36 (C≡C), 31.60, 31.44, 30.06, 30.00, 29.54, 29.30, 28.94, 28.78, 22.60, 22.48, 14.13, 14.08 (C_6H_{13}); FAB-MS: m/z 757.3 $[M]^+$. Anal. Calc. for $C_{49}H_{44}N_2S_3$: C, 77.74; H, 5.86; N, 3.70. Found: C, 77.54; H, 6.02; N, 3.89%.

The same procedure as **L1** was used to prepare **L2**.

L2: Orange solid (86%). *Spectral data*: IR (KBr): ν(C≡C) 2097 cm^{-1}; ^{1}H NMR (400 MHz, $CDCl_3$, δ/ppm): 8.87 (dd, $J_1 = 7.9$ Hz, $J_2 = 1.2$ Hz, 1H, Ar), 8.76 (d, $J = 8.5$ Hz, 1H, Ar), 8.72 (d, $J = 8.4$ Hz, 1H, Ar), 7.75 (t, $J = 7.0$ Hz, 1H, Ar), 7.69–7.65 (m, 1H, Ar), 7.53–7.36 (m, 4H, Ar), 7.25–7.14 (m, 6H, Ar), 7.09 (d, $J = 3.8$ Hz, 1H, Ar), 6.97 (s, 1H, Ar), 6.96 (d, $J = 3.8$ Hz, 1H, Ar), 6.79 (d, $J = 3.8$ Hz, 1H, Ar), 6.76 (s, 1H, Ar), 3.42 (s, 1H, C≡CH), 3.37 (s, 1H, C≡CH), 2.70 (t, $J = 7.8$ Hz, 2H, C_6H_{13}), 2.55 (t, $J = 7.7$ Hz, 2H, C_6H_{13}), 1.65–1.60 (m, 2H, C_6H_{13}), 1.44–1.38 (m, 8H, C_6H_{13}), 1.21–0.99 (m, 6H, C_6H_{13}), 0.89 (t, $J = 6.7$ Hz, 3H, C_6H_{13}), 0.76 (t, $J = 7.0$ Hz, 3H, C_6H_{13}); ^{13}C NMR (100 MHz, $CDCl_3$, δ/ppm): 145.93, 141.24, 140.80, 137.52, 137.43, 137.31, 136.04, 135.08, 134.53, 133.50, 133.41, 133.10, 130.90, 129.29, 129.45, 129.35, 129.21, 128.31, 127.93, 127.54, 127.46, 127.37, 127.17, 127.03, 126.99, 126.26, 125.69, 125.43, 125.39, 125.14, 124.07, 123.12, 122,76, 121.65, 121.61, 121.06 (Ar), 82.51, 82.43, 76.76, 76.71 (C≡C), 31.61, 31.39, 30.41, 30.33, 29.45, 29.21, 29.01, 22.59, 22.41, 14.10, 14.03 (C_6H_{13}); FAB-MS: m/z 921.4 $[M]^+$. Anal. Calc. for $C_{57}H_{48}N_2S_5$: C, 74.31; H, 5.25; N, 3.04. Found: C, 74.44; H, 5.12; N, 2.96%.

2.3.8. Synthesis of polymers *P1* and *P2*

The polymers were prepared by the dehydrohalogenative polycondensation between *trans*-Pt $(PBu_3)_2Cl_2$ and each of **L1**–**L2**. A typical procedure was given for **P1** starting from **L1**.

To a stirred solution mixture of **L1** (37 mg, 0.05 mmol) and *trans*-$Pt(PBu_3)_2Cl_2$ (33 mg, 0.05 mmol) in freshly distilled triethylamine (4 mL) and CH_2Cl_2 (4 mL) was added a small amount of CuI (3.00 mg). The solution was stirred at room temperature for 24 h under the nitrogen atmosphere. The solvents were removed on a rotary evaporator *in vacuo*. The residue was redissolved in CH_2Cl_2 and filtered through a short column on neutral aluminum oxide eluting with CH_2Cl_2 to remove ionic impurities and catalyst residue. After removal of the solvent, the crude product was precipitated in methanol from CH_2Cl_2. The precipitate was collected via filtration and washed with copious amounts of methanol and dried under vacuum for 5 h to afford the polymer **P1** (43 mg, 63%).

Spectral data: IR (KBr): ν(C≡C) 2083 cm^{-1}; ^{1}H NMR (400 MHz, $CDCl_3$, δ/ppm): 8.86 (t, $J = 7.6$ Hz, 1H, Ar), 8.78–8.70 (m, 2H, Ar), 7.73–7.65 (m, 2H, Ar), 7.52–7.50 (m, 1H, Ar), 7.42–7.40 (m, 1H, Ar), 7.36–7.31 (m, 2H, Ar), 7.20–7.13 (m, 4H, Ar), 7.04–7.00 (m, 1H, Ar), 6.81–6.77 (m, 1H, Ar), 6.63–6.58 (m, 1H, Ar), 2.59–2.53 (m, 2H, C_6H_{13}), 2.46–2.41 (m, 2H, C_6H_{13}), 2.10–2.07 (m, 3H, PBu_3), 1.76–1.74 (m, 6H, PBu_3), 1.50–1.43 (m, 8H, PBu_3), 1.30–1.09 (m, 33H, $PBu_3 + C_6H_{13}$), 0.94–0.86 (m, 9H, $PBu_3 + C_6H_{13}$), 0.84–0.80 (m, 13H, $PBu_3 + C_6H_{13}$), 0.74–0.70 (m, 4H, $PBu_3 + C_6H_{13}$); ^{31}P NMR (162 MHz, $CDCl_3$, δ/ppm): 3.04 ($^1J_{P-Pt} = 2336$ and 142 Hz); Anal. Calc. for $(C_{73}H_{96}N_2P_2S_3Pt)_n$: C, 64.72; H, 7.14; N, 2.07. Found: C, 64.97; H, 7.23; N, 2.32%; GPC (THF): $M_w = 76280$, $M_n = 35430$, DP = 26, PDI = 2.15.

P2: Orange solid (86%). *Spectral data*: IR (KBr): ν(C≡C) 2084 cm^{-1}; ^{1}H NMR (400 MHz, $CDCl_3$, δ/ppm): 8.88 (d, $J = 7.8$ Hz, 1H, Ar), 8.78 (d, $J = 8.5$ Hz, 1H, Ar), 8.73 (d, $J = 8.4$ Hz, 1H, Ar), 7.75 (t, $J = 7.5$ Hz, 1H, Ar), 7.67 (t, $J = 7.5$ Hz, 1H, Ar), 7.52–7.35 (m, 4H, Ar), 7.25–7.23 (m, 2H, Ar), 7.17–7.14 (m, 3H, Ar), 6.95–6.88 (m, 2H, Ar), 6.78–6.71 (m, 2H, Ar), 6.67–6.65 (m, 2H, Ar), 2.71–2.69 (m, 2H, C_6H_{13}), 2.64–2.48 (m, 2H, C_6H_{13}), 2.18–2.05 (m, 12H, PBu_3), 1.70–1.30 (m, 34H, $PBu_3 + C_6H_{13}$), 1.15–0.81 (m, 27H, $PBu_3 + C_6H_{13}$), 0.75 (t, $J = 7.0$ Hz, 3H, C_6H_{13}); ^{31}P NMR (162 MHz, $CDCl_3$, δ/ppm): 3.22 ($^1J_{P-Pt} = 2329$ Hz); Anal. Calc. for $(C_{81}H_{100}N_2P_2S_5Pt)_n$: C, 64.05; H, 6.64; N, 1.84. Found: C, 64.12; H, 6.76; N, 2.01%; GPC (THF): $M_w = 58370$, $M_n = 20910$, DP = 14, PDI = 2.79.

2.3.9. Synthesis of model complexes *M1* and *M2*

All of them were synthesized following the dehydrohalogenating coupling between *trans*-$Pt(PEt_3)_2(Ph)Cl$ and the corresponding diterminal alkynes. A typical procedure was given for **M1** starting from **L1**.

To a solution of ligand **L1** (7.0 mg, 0.01 mmol) and *trans*-$Pt(PEt_3)_2(Ph)Cl$ (11 mg, 0.02 mmol) in triethylamine (3 mL) and dry CH_2Cl_2 (3 mL) was added CuI (2 mg) under nitrogen. After stirring overnight at room temperature, all volatile components were removed under reduced pressure. The residue was dissolved in CH_2Cl_2 and purified by preparative silica TLC plates using CH_2Cl_2/hexane (1.8:1, v/v) as eluent to give the pure product **M1** as a red solid (8 mg, 43%).

Spectral data: IR (KBr): ν(C≡C) 2077 cm^{-1}; ^{1}H NMR (400 MHz, $CDCl_3$, δ/ppm): 8.87 (d, $J = 7.0$ Hz, 1H, Ar), 8.74 (d, $J = 8.4$ Hz, 1H, Ar), 8.68 (d, $J = 8.4$ Hz, 1H, Ar), 7.71 (d, $J = 7.3$ Hz, 1H, Ar), 7.64 (d, $J = 7.1$ Hz, 1H, Ar), 7.52–7.35 (m, 4H, Ar), 7.32–7.26 (m, 2H, Ar), 7.26–7.15 (m, 6H, Ar), 7.06 (s, 1H, Ar), 6.96 (t, $J = 7.4$ Hz, 2H, Ar), 6.88 (t, $J = 7.4$ Hz, 2H, Ar), 6.82 (s, 1H, Ar), 6.78 (t, $J = 7.3$ Hz, 1H, Ar), 6.74 (t, $J = 7.2$ Hz, 1H, Ar), 6.64 (s, 1H, Ar), 2.61 (t, $J = 7.6$ Hz, 2H, C_6H_{13}), 2.47 (t, $J = 7.6$ Hz, 2H, C_6H_{13}), 1.77–1.70 (m, 12H, PEt_3), 1.49–1.29 (m, 24H, $PEt_3 + C_6H_{13}$), 1.25–1.19 (m, 4H, C_6H_{13}), 1.12–1.05 (m, 18H, PEt_3), 0.96–0.76 (m, 24H, $PEt_3 + C_6H_{13}$); ^{31}P NMR (162 MHz, $CDCl_3$, δ/ppm): 10.16 ($^1J_{P-Pt} = 2635$ Hz), 9.63 ($^1J_{P-Pt} = 2626$ Hz); MALDI-TOF: m/z 1772.6440 $[M]^+$, Calculated: 1772.6320; Anal. Calc. For $C_{85}H_{112}N_2P_4S_3Pt_2$: C, 57.61; H, 6.37; N, 1.58. Found: C, 57.45; H, 6.46; N, 1.67%.

M2: Orange solid (49%). *Spectral data*: IR (KBr): ν(C≡C) 2081 cm^{-1}; ^{1}H NMR (400 MHz, $CDCl_3$, δ/ppm): 8.89 (d, $J = 8.0$ Hz, 1H, Ar), 8.78 (d, $J = 8.6$ Hz, 1H, Ar), 8.73 (d, $J = 8.2$ Hz, 1H, Ar), 7.74 (t, $J = 7.0$ Hz, 1H, Ar), 7.67 (t, $J = 7.0$ Hz, 1H, Ar), 7.53–7.49 (m, 1H, Ar), 7.47–7.26 (m, 7H, Ar), 7.25–7.23 (m, 2H, Ar), 7.17–7.14 (m, 3H, Ar), 6.99–6.93 (m, 5H, Ar), 6.89 (d, $J = 3.8$ Hz, 1H, Ar), 6.83–6.79 (m, 3H, Ar), 6.73 (d, $J = 3.8$ Hz, 1H, Ar), 6.68 (m, 2H, Ar), 2.71 (t, $J = 7.8$ Hz, 2H, C_6H_{13}), 2.55 (t, $J = 7.7$ Hz, 2H, C_6H_{13}), 1.78–1.64 (m, 26H, $PEt_3 + C_6H_{13}$), 1.40–1.32 (m, 8H, C_6H_{13}), 1.15–1.02 (m, 42H, $PEt_3 + C_6H_{13}$), 0.90 (t, $J = 6.8$ Hz, 3H, C_6H_{13}), 0.76 (t, $J = 7.0$ Hz, 3H, C_6H_{13}); ^{31}P NMR (162 MHz, $CDCl_3$, δ/ppm): 9.98, 9.95 ($^1J_{P-Pt} = 2631$ Hz); MALDI-TOF: m/z 1935.3507 $[M]^+$, Calculated: 1935.6000; Anal. Calc. For $C_{93}H_{116}N_2P_4S_5Pt_2$: C, 57.69; H, 6.04; N, 1.45. Found: C, 57.98; H, 6.15; N, 1.30%.

2.4. Solar cell fabrication and characterization

The device structure was ITO/PEDOT:PSS/polymer:PCBM blend/Al. The ITO glass substrates (10 Ω per square) were cleaned by sonication in toluene, acetone, ethanol and deionized water, dried in an oven, and then cleaned with UV ozone for 300 s. As-received PEDOT:PSS solution was passed through the 0.45 μm filter and spin-coated on patterned ITO substrates at 5000 r.p.m. for 3 min, followed by baking in N_2 at 150 °C for 15 min. The polymer:PCBM

(1:4 by weight) active layer was prepared by spin-coating the chlorobenzene solution (30 mg per mL) at 800 r.p.m. for 2 min. The substrates were dried at room temperature in low vacuum (vacuum oven) for 1 h, and then stored in high vacuum (10^{-5}–10^{-6} Torr) overnight. Al electrode (100 nm) was evaporated through a shadow mask to define the active area of the devices (2 mm diameter circle). All the fabrication procedures (except drying, PEDOT:PSS annealing and Al deposition) and cell characterization were performed in air. Power conversion efficiency was determined from *J*–*V* curve measurement (using a Keithley 2400 sourcemeter) under white light illumination (at 100 mW cm^{-2}). For white light efficiency measurements, Oriel 66002 solar light simulator with AM 1.5 filter was used. The light intensity was measured by a Molectron Power Max 500D laser power meter.

3. Results and discussion

3.1. Synthetic methodologies and chemical characterization

The chemical structures and synthesis of new platinum(II) polyyne polymers **P1**–**P2** and their model compounds **M1**–**M2** are shown in Scheme 1. In the initial attempt, we tried to synthesize the compound **PITBr** according to the method reported in the literature [22], that is, ring closure reaction followed by bromination, but unfortunately we failed in the second step and it was messy and difficult to separate the target product from the reaction mixture. So, we optimized the synthetic methods as follows. Thiophene-3-carboxaldehyde was first brominated by bromine in the solvent mixture of 48% aqueous hydrobromic acid and diethyl ether to give 2,5-dibromo-3-formylthiophene. The ring closure reaction between phenanthrenequinone, 2,5-dibromo-3-formylthiophene and aniline was carried out in the presence of ammonium acetate and acetic acid to achieve the key precursor **PITBr** as a yellow solid. Following Stille cross-coupling reaction and bromination with *N*-bromosuccinimide (NBS), compound **L1**-**Br** was obtained in high yield. Repeating the similar Stille cross-coupling reaction, **L2**-**T** was obtained and sequential bromination gave compound **L2**-**Br**. By Sonogashira coupling reaction, the bromide groups were converted to the corresponding trimethylsilylethynyl groups in a CH_2Cl_2/NEt_3 mixture using CuI, $Pd(OAc)_2$ and PPh_3 as the catalysts. Following desilylation with potassium carbonate in methanol, the final diethynyl ligands **L1**–**L2** were obtained as orange solids. Polymers **P1**–**P2** and their model compounds **M1**–**M2** were prepared by the Sonogashira-type dehydrohalogenation between each of the diethynyl precursors and the corresponding platinum precursors *trans*-$Pt(PBu_3)_2Cl_2$ and *trans*-$Pt(PEt_3)_2(Ph)Cl$ with the stoichiometric ratio of 1:1 and 1:2.1, respectively. Polymers **P1**–**P2** were purified by flash column chromatography over neutral Al_2O_3 to remove ionic impurities and catalyst residues, and repeated precipitation and isolation.

All of the Pt compounds are thermally- and air-stable solids and they are soluble in common chlorinated hydrocarbons. From the gel permeation chromatography (GPC) analysis on **P1** and **P2**, the number-average molecular weights (M_n) of **P1** and **P2** calibrated against polystyrene standards were 3.54 and 2.09 kg mol^{-1}, corresponding to the polydispersity indices (PDI) of 2.15 and 2.79, indicating that **P1** and **P2** possess 26 and 14 repeating units, respectively. The structures of polymers **P1**–**P2** and their model compounds **M1**–**M2** were unequivocally characterized using mass spectrometry, IR and NMR spectroscopies (see Experimental section). The NMR data are consistent with the proposed structure of the polymers and model compounds. The peaks arising from terminal –C≡CH groups are absent in the NMR and IR spectra, confirming metal–alkynyl bond formation.

The thermal properties of the polymers were also examined by thermal gravimetric analysis (TGA) under nitrogen. Polymer **P1** exhibits good thermal stability with the decomposition onsets at ~339 °C and the percent weight loss is ~15%, indicating that two butyl groups were removed from the polymer. For polymer **P2**, two butyl groups were removed at the lower decomposition temperature of 238 °C, while elevating the temperature up to 374 °C, six butyl groups were all removed from polymer, as deduced from the percentage weight loss of ~23% as shown in the TGA curve.

3.2. Photophysical and electrochemical characterization

The absorption and emission spectra of the ligands, polymers and model complexes were measured in CH_2Cl_2 solutions at 293 K (Table 1 and Figs. 1 and 2). All the compounds show two absorption bands, one sharp and strong peak at about 260 nm and the other broad and relatively weak peak between 320 and 550 nm [22–24]. The former is caused by the presence of conjugated phenanthrenyl-imidazole moieties that are not fully coplanar to the thiophene polymer main chain because of the steric hindrance. The latter is assigned to the π–π^* transitions of the conjugated chain [22–24] and the presence of the phenanthrenyl-imidazole moieties increases the effective conjugation length of the polythiophene main chain to some extent. With the extension of the π-conjugation system, the second absorption band becomes gradually stronger and red-shifted to the longer wavelength, as revealed by a comparison of the absorption spectra of the diethynyl ligands and the corresponding platinum(II) complexes. Besides, the maximum absorption peak of **L2** is shown at 424 nm, and an obvious red shift of 28 nm occurs compared with that of **L1** at 396 nm, probably because the introduction of additional thiophene rings results in the extension of the π-conjugated system. While **M1** and **M2** show the same absorption peak at 449 nm, **P2** shows a slightly blue-shifted absorption band compared with that of **P1**. We speculate that the blue-shifted absorption peak may be related to the lower molecular weight and lower degree of polymerization for **P2**. The optical band gaps of **P1** and **P2** are 2.34 and 2.28 eV, respectively. Presumably, a higher degree of conjugation with the additional thienyl units reduces the band gap.

All the phenanthrenyl-imidazole-based diethynyl ligands, model complexes and polymers show photoluminescence properties in the visible region. Polymers **P1** and **P2** can emit intense fluorescence from the singlet excited states at 531 and 560 nm, respectively, and show a significant red shift compared to the corresponding ligands **L1** and **L2** at 484 and 527 nm, respectively, which indicates the longer length of π-conjugation. The emission properties of **M1**–**M2** are very similar to those of **P1**–**P2**, with the emission maxima at 516 and 562 nm, respectively. The measured photoluminescence lifetimes for these compounds are very short (ca. 0.70–2.27 ns), characteristic of the spin-allowed singlet emission. These results and the small Stokes shift preclude the emitting state as a triplet but a singlet excited state instead [32,49]. In addition, the emission density of ligands, dimers and polymers decreased gradually with the extended π-conjugation length, as deduced from the reduced quantum yield values. Therefore, it is mostly an intramolecular charge transfer (ICT) excited state that contributes to the effective photoinduced charge separation in energy conversion for **P1**–**P2** [36,49].

The highest occupied molecular orbital (HOMO) and the lowest unoccupied molecular orbital (LUMO) levels of stable **P1**–**P2** were determined from electrochemical measurements using cyclic voltammetry. The experiments were performed by casting the polymer films on the glassy-carbon working electrode with a Ag/AgCl wire as the reference electrode, at a scan rate of 100 mV s^{-1}. The solvent in all measurements was deoxygenated acetonitrile, and

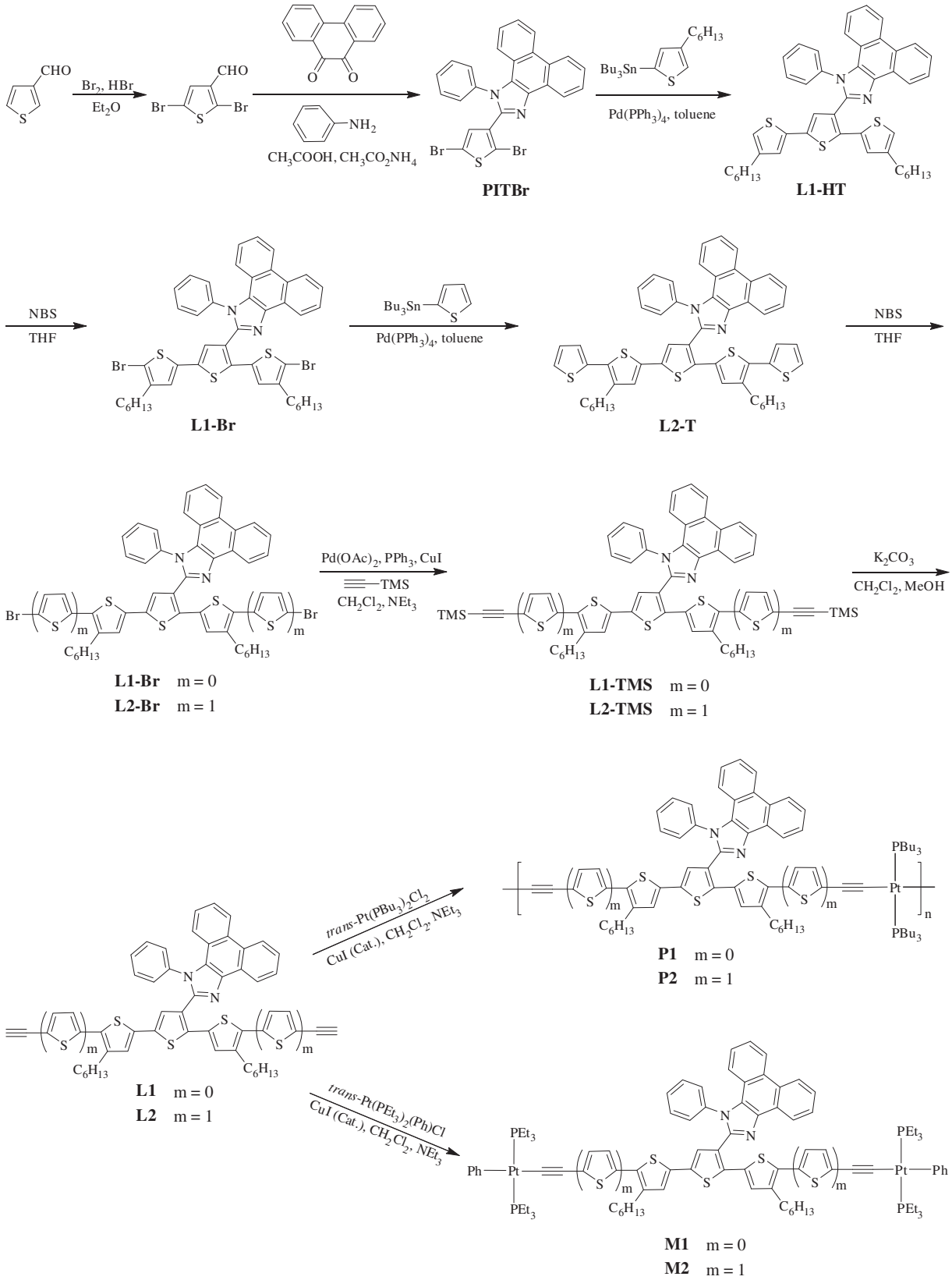

Scheme 1. Chemical structures and synthetic pathways of **P1**–**P2** and **M1**–**M2**.

Table 1
Absorption and emission data for diethynyl ligands **L1**–**L2**, model complexes **M1**–**M2** and polymers **P1**–**P2**.[a]

	λ_{abs} [nm] ($\varepsilon \times 10^4$ M^{-1} cm^{-1})	λ_{emi} [nm] (τ_F, ns)	Φ_F (%)
L1	259 (4.9), 396 (1.7)	484 (0.70)	4.46
L2	259 (5.7), 424 (2.7)	527 (1.18)	13.40
M1	260 (5.4), 449 (2.8)	516 (1.18), 539 (1.11)	3.62
M2	260 (4.9), 449 (2.7)	562 (0.99)	9.79
P1	259, 466	531 (0.92), 552 (2.09)	1.03
P2	259, 459	560 (2.27)	3.40

[a] All the photophysical data were measured in CH_2Cl_2 at 293 K; Quantum yields were measured with an excitation wavelength of 420 nm using coumarin 6 in ethanol as the reference ($\Phi_F = 0.78$).

the supporting electrolyte was 0.1 M [^{n}Bu$_4$N]BF$_4$. The relevant data are collected in Table 2. From the values of reduction potential (E_{red}), the LUMO levels of **P1**–**P2** were calculated according to the following equations $E_{LUMO} = -(E_{red} + 4.72)$ eV (where the unit of potential is V vs. Ag/AgCl) and $E_{HOMO} = -(E_g^{opt} - E_{LUMO})$ eV. Polymers **P1** and **P2** show a quasi-reversible reduction wave at −0.81 and −0.87 V, respectively, which is attributed to the reduction of the phenanthrenyl-imidazole moiety. The HOMO level of **P2** is −6.13 eV, which is higher than that of **P1** (−6.25 eV), and the HOMO energy levels are elevated with the enhanced electron-donating ability of the donor units.

3.3. Polymer solar cell behavior

Since the generated excitons could readily dissociate into electrons and holes and transfer from the electron-donating polymeric main chain to the electron-withdrawing moieties in the side-chain-tethered phenanthrenyl-imidazole conjugated polymers, which favors the photocurrent generation and photoelectronic energy conversion in photovoltaic devices, polymer solar cells were fabricated by using **P1** and **P2** as the electron donor and PCBM as the electron acceptor with a blend ratio of 1:4. The hole-collection electrode consisted of indium tin oxide (ITO) with a spin-coated poly(3,4-ethylene-dioxythiophene)/poly(styrene sulfonate) (PEDOT/PSS) layer, whereas Al served as the electron-collecting electrode. The current density (J) vs. voltage (V) curves of the solar cells with the blend layer of **P1**/PCBM and **P2**/PCBM (1:4) are shown in Fig. 3. The open-circuit voltage (V_{oc}), short-circuit current density (J_{sc}), fill factor (FF), and PCE of the devices are summarized in Table 2.

The higher PCE of 0.39% for this type of polymers was obtained by the device using **P2**/PCBM (1:4) as the active layer with a V_{oc} of 0.53 V, a J_{sc} of 2.67 mA cm^{-2} and an FF of 0.28, while the device based on **P2**/PCBM (1:4) shows a PCE of 0.28% with a V_{oc} of 0.58 V, a J_{sc} of 1.44 mA cm^{-2} and an FF of 0.33 under the same conditions, mainly due to the higher J_{sc} for **P2** which is almost double that of **P1**. It is known that the ICT effect can be strengthened with the enhancement of electron-donating ability of donor unit or electron-withdrawing ability of acceptor [50,51]. Therefore, the addition of thiophene unit in **P2** could result in more rapid charge transfer from the polymeric main chain to the electron-withdrawing phenanthrenyl-imidazole-tethered side chains and then to PCBM [23]. **P2** has a relatively lower V_{oc} than that of **P1**, which is consistent with its higher HOMO energy value, because V_{oc} is linearly correlated with the difference of the HOMO energy level of the donor and the LUMO energy level of the acceptor [52]. Among them, the FFs are relatively lower than those of higher

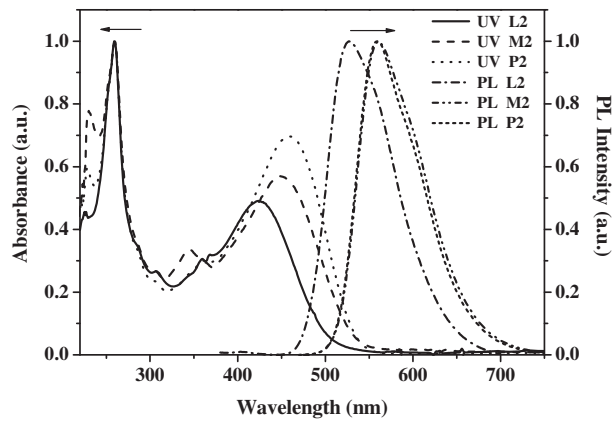

Fig. 2. Normalized absorption and emission spectra of **L2**, **M2** and **P2** in CH_2Cl_2 at 293 K.

Table 2
Electrochemical data and photovoltaic performances for polymers **P1**–**P2**.[a]

Polymer	E_g^{opt} (eV)	E_{red}/E_{LUMO} (V)/(eV)	E_{HOMO} (eV)	V_{oc} (V)	J_{sc} (mA cm^{-2})	FF	PCE (%)
P1	2.34	−0.81/−3.91	−6.25	0.58	1.44	0.33	0.28
P2	2.28	−0.87/−3.85	−6.13	0.53	2.67	0.28	0.39

[a] $E_g^{opt} = 1240/\lambda_{onset}$ where λ_{onset} is the onset value of absorption spectrum in CH_2Cl_2; $E_{LUMO} = -(E_{red} + 4.72)$ eV; $E_{HOMO} = -(E_g^{opt} - E_{LUMO})$ eV.

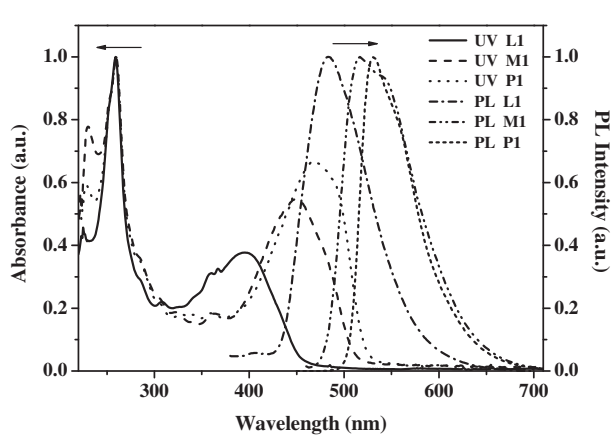

Fig. 1. Normalized absorption and emission spectra of **L1**, **M1** and **P1** in CH_2Cl_2 at 293 K.

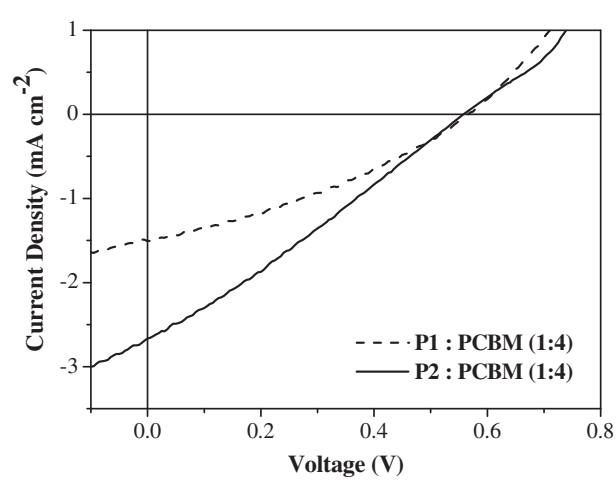

Fig. 3. J–V curves of solar cell devices with **P1** and **P2**:PCBM (1:4) active layers under AM 1.5 G illumination.

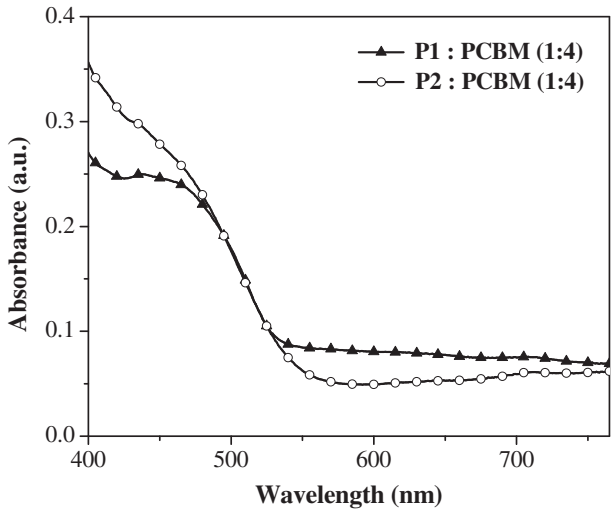

Fig. 4. Absorption spectra for solar cell devices based on **P1** and **P2**:PCBM (1:4) blends.

performance polymers reported before, partly due to the fact that all processing (except PEDOT:PSS annealing and electrode deposition) and measurements have been done in ambient atmosphere which likely results in the presence of traps. So, we expect FF to improve for fabrication and characterization to be performed in an inert gas environment. Comprehensive study of charge transport and the influence of traps is necessary to further improve FF and overall device performance. It is worth mentioning that the photovoltaic efficiency of **P1** device was improved to 0.79% when $PC_{70}BM$ was used as the electron acceptor to optimize the device, which represents a two-fold increase than that of the **P1**/PCBM device.

The absorption spectra of **P1**:PCBM and **P2**:PCBM (1:4) blend films prepared under the same conditions are shown in Fig. 4, and the EQE curves for these devices are depicted in Fig. 5. The shapes of EQE curves of these polymers are similar to their corresponding UV/vis absorption spectra, illustrating that all the light energy absorbed by the polymer/PCBM blend film is to some extent converted into electricity. The blend films only have relatively strong absorption between 400 and 535 nm mainly arising from the organometallic polymers. The limited absorption results in the low PCE for this kind of polymers. The maximum EQE values for **P1** and **P2** devices reach 13% and 21% at an incident wavelength of 455 nm, respectively.

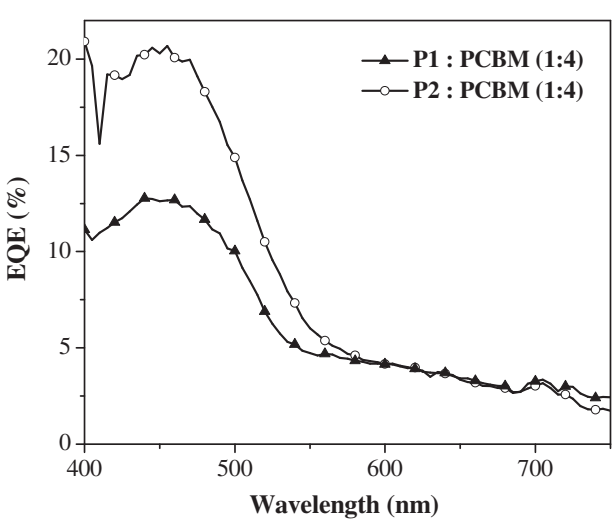

Fig. 5. EQE spectra for solar cell devices based on **P1** and **P2**:PCBM (1:4) blends.

4. Conclusions

In summary, two new D–A side-chain-tethered phenanthrenyl-imidazole platinum(II) polyyne polymers were synthesized and characterized. These polymers exhibit a narrow and strong band around 260 nm and a broad lower energy absorption band in the visible region. The optical band gaps range from 2.28 eV to 2.34 eV. The incorporation of additional thiophene fragments into the polymer chain improves the ICT effect in the D–A π-conjugation system, which results in higher $J_{sc,}$ and thus improves the performance of the resulting PSCs to 0.39%. One of the major limiting parameters is presumably due to the restricted absorption properties in the visible region. Therefore, it is expected that a continuous optimization of the chemical structures of polymer main chain by incorporating some special functional chromophores with stronger electron-donating ability than thiophene rings or the phenanthrenyl-imidazole side chain modified by strong electron-withdrawing groups such as F or CF_3 would narrow the band gaps and thus enhance the photovoltaic efficiency of this kind of metallopolymers.

Acknowledgements

This work was supported by the University Grants Committee Areas of Excellence Scheme (AoE/P-03/08), the Faculty Research Grant from Hong Kong Baptist University (FRG2/09-10/091), the General Research Fund (HKBU202607) as well as the Collaborative Research Fund (HKUST2/CRF/10) from the Hong Kong Research Grants Council. This work was also partly supported by Strategic Research Theme and University Development Fund of the University of Hong Kong.

References

[1] J.Y. Kim, K. Lee, N.E. Coates, D. Moses, T.Q. Nguyen, M. Dante, A.J. Heeger, Science 317 (2007) 222.
[2] S. Gunes, H.S. Neugebauer, N.S. Sariciftic, Chem. Rev. 107 (2007) 1324.
[3] B.C. Thompson, J.M.J. Fréchet, Angew. Chem. Int. Ed. 47 (2008) 58.
[4] R. Po, M. Maggini, N. Camaioni, J. Phys. Chem. C 114 (2010) 695.
[5] Y.J. Cheng, S.H. Yang, C.S. Hsu, Chem. Rev. 109 (2009) 5868.
[6] H.-Y. Chen, J.H. Hou, S.Q. Zhang, Y.Y. Liang, G.W. Yang, Y. Yang, L.P. Yu, Y. Wu, G. Li, Nat. Photonics 3 (2009) 649.
[7] C. Piliego, T.W. Holcombe, J.D. Douglas, C.H. Woo, P.M. Beaujuge, J.M.J. Fréchet, J. Am. Chem. Soc. 132 (2010) 7595.
[8] C.J. Brabec, N.S. Sariciftci, J.C. Hummelen, Adv. Funct. Mater. 11 (2001) 15.
[9] S.C. Ng, H.-F. Lu, H.S.O. Chan, A. Fujii, T. Laga, K. Yoshino, Adv. Mater. 12 (2000) 1122.
[10] T. Yoshihara, S.I. Druzhinin, K.A. Zachariasse, J. Am. Chem. Soc. 126 (2004) 8535.
[11] A. Escosura, M.V. Martinez-Diaz, D.M.G.T. Torres, J. Am. Chem. Soc. 128 (2006) 4112.
[12] E.H.A. Beckers, S.C.J. Meskers, A.P.H.J. Schenning, Z. Chen, F. Würthner, P. Marsal, D. Beljonne, J. Cornil, R.A.J. Janssen, J. Am. Chem. Soc. 128 (2006) 649.
[13] A.M. Ramos, S.C.J. Meskers, E.H.A. Beckers, R.B. Prince, L. Brunsveld, R.A.J. Janssen, J. Am. Chem. Soc. 126 (2004) 9630.
[14] R. Gaudiana, C. Brabec, Adv. Mater. 18 (2006) 2884.
[15] E.G. Wang, L. Wang, L.F. Lan, C. Luo, W.L. Zhuang, J.B. Peng, Y. Cao, Appl. Phys. Lett. 92 (2008) 033307.
[16] N. Blouin, A. Michaud, D. Gendron, S. Wakim, E. Blair, R. Neagu-Plesu, M.B. Te, G. Durocher, Y. Tao, M. Leclerc, J. Am. Chem. Soc. 130 (2008) 732.
[17] N.S. Baek, S.K. Hau, H.-L. Yip, O. Acton, K.-S. Chen, A.K.-Y. Jen, Chem. Mater. 20 (2008) 5734.
[18] J. Hou, H.Y. Chen, S. Zhang, G. Li, Y. Yang, J. Am. Chem. Soc. 130 (2008) 16144.
[19] S.H. Park, A. Roy, S. Beaupre, S. Cho, N. Coates, J.S. Moon, D. Moses, M. Leclerc, K. Lee, A.J. Heeger, Nat. Photonics 3 (2009) 297.
[20] Y.Y. Liang, D.Q. Feng, Y. Wu, S.T. Tsai, G. Li, C. Ray, L.P. Yu, J. Am. Chem. Soc. 131 (2009) 7792.
[21] J. Peet, J.Y. Kim, N.E. Coates, W.L. Ma, D. Moses, A.J. Heeger, G.C. Bazan, Nat. Mater. 6 (2007) 497.

[22] Y.-T. Chang, S.-L. Hsu, M.-H. Su, K.-H. Wei, Adv. Funct. Mater. 17 (2007) 3326.
[23] Y.-T. Chang, S.-L. Hsu, G.Y. Chen, M.-H. Su, T.A. Singh, E.W.G. Diau, K.-H. Wei, Adv. Funct. Mater. 18 (2008) 2356.
[24] Y.-T. Chang, S.-L. Hsu, M.-H. Su, K.-H. Wei, Adv. Mater. 21 (2009) 2093.
[25] M.-C. Yuan, M.-H. Su, M.-Y. Chiu, K.-H. Wei, J. Polym. Sci., Part A: Polym. Chem. 48 (2010) 1298.
[26] F. Huang, K.-S. Chen, H.-L. Yip, S.K. Hau, O. Acton, Y. Zhang, J. Luo, A.K.-Y. Jen, J. Am. Chem. Soc. 131 (2009) 13886.
[27] F. Giacalone, J.L. Segura, N. Martin, M. Catellani, S. Luzzati, N. Lupsac, Org. Lett. 5 (2003) 1669.
[28] H. Masai, K. Sonogashira, N. Hagihara, Bull. Chem. Soc. Jpn. 44 (1971) 2226.
[29] H.F. Wittmann, K. Fuhrmann, R.H. Friend, M.S. Khan, J. Lewis, Synth. Met 55 (1993) 56.
[30] J. Lewis, M.S. Khan, B.F.G. Johnson, T.B. Marder, H.B. Fyfe, H.F. Wittmann, R.H. Friend, A.E. Dray, J. Organomet. Chem. 425 (1992) 165.
[31] J.S. Wilson, N. Chawdhury, M.R.A. Al-Mandhary, M. Younus, M.S. Khan, P.R. Raithby, A. Köhler, R.H. Friend, J. Am. Chem. Soc. 123 (2001) 9412.
[32] W.-Y. Wong, C.L. Ho, Coord. Chem. Rev. 250 (2006) 2627.
[33] W.-Y. Wong, Dalton Trans. (2007) 4495.
[34] W.-Y. Wong, P.D. Harvey, Macromol. Rapid Commun. 31 (2010) 671.
[35] A. Kohler, H.F. Wittmann, R.H. Friend, M.S. Khan, J. Lewis, Synth. Met. 67 (1994) 245.
[36] W.-Y. Wong, X.Z. Wang, Z. He, A.B. Djurišić, C.T. Yip, K.Y. Cheung, H. Wang, C.S.K. Mak, W.K. Chan, Nat. Mater. 6 (2007) 521.
[37] W.-Y. Wong, C.-L. Ho, Acc. Chem. Res. 43 (2010) 1246.
[38] W.-Y. Wong, Macromol. Chem. Phys. 209 (2008) 14.
[39] W.-Y. Wong, X.Z. Wang, Z. He, K.-K. Chan, A.B. Djurišić, K.Y. Cheung, C.T. Yip, AM.-C. Ng, Y.Y. Xi, C.S.K. Mak, W.-K. Chan, J. Am. Chem. Soc. 129 (2007) 14372.
[40] L. Liu, C.-L. Ho, W.-Y. Wong, K.-Y. Cheung, M.-K. Fung, W.-T. Lam, A.B. Djurišić, W.-K. Chan, Adv. Funct. Mater. 18 (2008) 2824.
[41] X.Z. Wang, W.-Y. Wong, K.-Y. Cheung, M.-K. Fung, A.B. Djurišić, W.-K. Chan, Dalton Trans. (2008) 5484.
[42] X.Z. Wang, Q.W. Wang, L. Yan, W.-Y. Wong, K.-Y. Cheung, A. Ng, A.B. Djurišić, W.-K. Chan, Macromol. Rapid Commun. 31 (2010) 861.
[43] Q.W. Wang, W.-Y. Wong, Polym. Chem. 2 (2011) 432.
[44] J. Chatt, B.L. Shaw, J. Chem. Soc. (1959) 4020.
[45] G.B. Kauffman, L.A. Teter, Inorg. Synth. 7 (1963) 245.
[46] G.A. Reynolds, K.H. Drexhage, Opt. Commun. 13 (1975) 222.
[47] S.A. Miehlich, H. Stoll, H. Preuss, Chem. Phys. Lett. 157 (1989) 200.
[48] J.S. Binkley, J.A. Pople, W.J. Hehre, J. Am. Chem. Soc. 102 (1980) 939.
[49] M. Younus, A. Köhler, S. Cron, N. Chawdhury, M.R.A. Al-Mandhary, M.S. Khan, J. Lewis, N.J. Long, R.H. Friend, P.R. Raithby, Angew. Chem. Int. Ed. 37 (1998) 3036.
[50] Y.W. Li, H. Li, B. Xu, Z.F. Li, F.P. Chen, D.Q. Feng, J.B. Zhang, W.J. Tian, Polymer 51 (2010) 1786.
[51] P.T. Wu, F.S. Kim, R.D. Champion, S.A. Jenekhe, Macromolecules 4 (2008) 7021.
[52] M.C. Scharber, D. Muhlbacher, M. Koppe, P. Denk, C. Waldauf, A.J. Heeger, C.J. Brabec, Adv. Mater. 18 (2006) 789.